

ALMA memo 515

Calculation of integration times for WVR

Alison Stirling, Mark Holdaway, Richard Hills, John Richer

March 2, 2005

1 Abstract

In this memo we address the issue of how to apply water vapour radiometer estimates of atmospheric phase to visibility data. We consider the impact of smoothing the radiometer data over a period of time to reduce the noise in the w.v.r. estimate, and applying a multiplicative factor to decrease the impact of the w.v.r. estimate when the phase fluctuation amplitude is small compared with the radiometer noise.

We find that when fast-switching is taken into account, for fully three-dimensional turbulence, and r.m.s. path length fluctuations of order $75 \mu\text{m}$, the optimal smoothing timescale is 11 seconds. This timescale decreases to around 3 seconds as the thickness of the turbulence layer becomes small compared with the baseline length. These values are found to decrease as the r.m.s. fluctuations increase. A multiplicative factor is required to modify the w.v.r. correction term for fluctuations less than $\sim 50 \mu\text{m}$, where the noise in the radiometer becomes comparable to fluctuations at the site.

2 Introduction

At Chajnantor, the atmosphere is expected to give rise to refractive index fluctuations due to inhomogeneities in the water vapour and air density distribution. These are expected to produce phase fluctuations corresponding to $70\text{-}600 \mu\text{m}$ of path, (or 1-8 degrees on a 300 m baseline at 11.2 GHz) (Butler *et al.* 2001, memo 365; Evans *et al.* 2003, memo 471), and if uncorrected can give rise to image artefacts as well as significantly reducing the sensitivity of the interferometer. There are two main methods for correcting for the effects of atmospheric phase – fast switching, which is sensitive to the total atmospheric phase, but along the line of sight to the calibrator, and water vapour radiometry (w.v.r.), which measures the fluctuations in water vapour along the line of sight to the source. The two methods are expected to have complementary roles in the phase correction process.

In this memo we consider how best to apply the w.v.r. phase correction. The raw w.v.r. phase estimate contains a contribution from thermal noise in the radiometer (Hills, 2004; memo 495) as well as an error arising from uncertainty in the conversion between bright-

ness temperature and atmospheric phase, which is dependent on the atmospheric conditions (Stirling *et al.*, 2004; memo 496). Clearly if the atmospheric phase correction required is very small, the thermal noise contribution can dominate the atmospheric signal, and in these circumstances simple subtraction of the w.v.r.-measured phase may add more phase noise to the visibilities than it removes. In these cases a different strategy is required for applying the phase, for instance by applying only a fraction of the w.v.r.-derived phase. A similar technique could also be used when there is some correlation between the dry and wet phase terms, allowing the phase estimate to be increased or decreased accordingly. The noise contribution from the w.v.r. can also be decreased by integrating the w.v.r. measurements over a longer time-period. On timescales up to ten seconds (Williamson, 2004), the noise is expected to scale inversely with the square root of the integration time. Increasing the integration time, however, also reduces the w.v.r.'s sensitivity to small-scale water vapour fluctuations, and so the choice of appropriate timescale will depend both on the statistics of the atmospheric fluctuations, and the amplitude of the noise component.

In this memo we calculate the integration times and multiplicative factor that will give the best estimate for the visibility given the expected levels of radiometer noise, and typical atmospheric fluctuations. The atmospheric phase fluctuations are treated as a random Gaussian process with a Kolmogorov power spectrum on small scales.

The layout of this report is as follows: Section 3 provides a brief context to the phase correction problem, and Section 4 outlines the mathematical formalism used to calculate the optimum integration time and multiplicative factor. In Section 5 we calculate the expected form of the phase structure function, taking into account the size of the antenna, and the effect of fast switching. The resulting optimum integration time-scales are presented in Section 6, using some typical numbers for the statistics of phase fluctuations at Chajnantor. The findings are summarised in Section 7.

3 Visibility measurements

ALMA is expected to produce several visibility measurements a second, and if phase switching is used to eliminate small offsets in the correlator outputs, these will be averaged into bundles of about one second (or 16 ms times the number of antennas; Thompson, Moran & Swenson, 2001). The w.v.r. correction is then applied to these averaged measurements before the visibilities are gridded up in the $u - v$ plane. We outline how this might work below.

Suppose we measure a series of complex visibilities, V_i . Each visibility contains the astronomical visibility, V_{ast} , (*i.e.* the quantity we want to know), a shift in phase due to the atmosphere θ_i^{atmos} , and a complex contribution from instrument noise, \mathcal{N}_i . We can write the measured visibility as:

$$V_i = V_{\text{ast}} \exp[i\theta_i^{\text{atmos}}] + \mathcal{N}_i. \quad (1)$$

If phase switching is used, the visibilities are averaged over a timescale η , which may be

of order 1 second, and so the visibility data obtained is given by:

$$V_j^\eta = \frac{1}{N} \sum_{i=(j-1)N}^{jN} \left[V_{\text{ast}} \exp[i\theta_i^{\text{atmos}}] + \mathcal{N}_i \right], \quad (2)$$

where N is the number of visibility measurements in the time period η . Now for short timescales of η (up to a few seconds), the variance in θ_i^{atmos} is small enough that $\sin(\Delta\theta_i^{\text{atmos}}) \simeq \Delta\theta_i^{\text{atmos}}$, and $\cos(\Delta\theta_i^{\text{atmos}}) \simeq 1$, and we can say:

$$V_j^\eta \simeq V_{\text{ast}} \exp[i\theta_j^\eta] + \mathcal{N}_j^\eta, \quad (3)$$

where $\theta_j^{\eta \text{atmos}}$ is just θ_i^{atmos} averaged over the time interval η , and similarly for \mathcal{N}_j^η .

Now for each visibility measurement, V_j^η , we have a corresponding estimate for the atmospheric phase, ϕ_j^{wvr} . Our estimate for the corrected visibility, \tilde{V}_j^η , is therefore:

$$\begin{aligned} \tilde{V}_j^\eta &= V_j^\eta e^{-i\phi_j^{\text{wvr}}} \\ &= V_{\text{ast}} \exp[i\theta_j^{\eta \text{atmos}} - i\phi_j^{\text{wvr}}] + \mathcal{N}_j^\eta \exp[-i\phi_j^{\text{wvr}}]. \end{aligned} \quad (4)$$

The visibilities are averaged further when the data is gridded into separate (u, v) cells, and so our final estimate for the visibility at a given (u, v) cell is given by:

$$\tilde{V}(u, v) = \frac{1}{N_g} \sum_{j=1}^{N_g} V_{\text{ast}} \exp[i\theta_j^{\eta \text{atmos}} - i\phi_j^{\text{wvr}}] + \frac{1}{N_g} \sum_{j=1}^{N_g} \mathcal{N}_j^\eta \exp[-i\phi_j^{\text{wvr}}], \quad (5)$$

where N_g is the number of visibility measurements lying in the grid-cell (u, v) . The timescale over which the visibilities can be gridded to form a single (u, v) coordinate is set by the time taken for the earth's rotation to move the dishes by about half the diameter of the dish ($D/2$). If we consider that the longest baseline (of length b) traces out a circle in the $u - v$ plane as seen from the south-pole, then the time taken to move by $D/2$, is

$$t = \frac{12 \text{ hours } D}{\pi 2b}. \quad (6)$$

For a baseline of 20 km, the maximum averaging time is 4 s, while for a baseline of 0.2 km, the maximum averaging time is 400 s, and so for $\eta \simeq 1$ s, N_g is likely to range between 4 and 400.

Since the noise term is uncorrelated with the atmospheric phase, the best approximation for V_{ast} can be obtained when N_g is maximum (since the noise decreases as the square root of N_g), and by minimising the contribution from the atmospheric exponent *i.e.* minimising $(\theta_j^{\eta \text{atmos}} - \phi_j^{\text{wvr}})^2$. In this memo, we concentrate on producing the best estimate for the atmospheric phase from the w.v.r. so that $(\theta_j^{\eta \text{atmos}} - \phi_j^{\text{wvr}})^2$ is minimised. The w.v.r. estimate for atmospheric phase is also affected by noise in the radiometer, and so we can aim to reduce its contribution by averaging the w.v.r. estimate for the atmospheric phase over a longer period of time. Clearly, the longer the time of integration, the smoother the atmospheric background appears, but the lower the noise contribution.

We can also introduce a multiplicative factor, α , which allows the correction term to be reduced when the noise becomes large compared with the atmospheric phase fluctuations, and which can increase the correction term when the smoothing has reduced the power in that term. In the next section, we calculate an expression for the optimum integration time and multiplicative factor α .

4 Calculation of integration times

In this section we calculate an expression for the time interval over which the radiometer phase data needs to be averaged, and the corresponding optimal value for the multiplicative factor, α , to give the best estimate for the atmospheric phase.

Since the visibilities are initially averaged over a given time interval, η , we let θ_η be the true atmospheric phase at time t averaged over a time interval of length η , so that $-\eta/2 < t < \eta/2$. ϕ_τ is the w.v.r. estimated phase averaged over a time interval τ . n_τ is the radiometer noise, also averaged over the time interval τ .

It is worth noting that the timescale η (*i.e.* the visibility integration time) is set by the way ALMA processes the data, and tends to be small (of order 1 s) and that this timescale in the atmospheric phase is preserved even if the visibilities are then smoothed over some other timescale. Conversely, the time scale τ , is a quantity we are free to change because the w.v.r. phase is estimated explicitly. The aim of this work is to calculate how long τ should be so as to minimise the noise component, while keeping the most accurate phase correction. We can cast this as a minimisation of the quantity ϵ_τ , where:

$$\epsilon_\tau^2 = \langle (\theta_\eta - \alpha\phi_\tau - \alpha n_\tau)^2 \rangle \quad (7)$$

and the angle brackets represent an average over time, and α is a constant that we are free to choose. We can expand this to be:

$$\epsilon_\tau^2 = \langle \theta_\eta^2 \rangle + \alpha^2 \langle \phi_\tau^2 \rangle + \alpha^2 \langle n_\tau^2 \rangle - 2\alpha \langle \theta_\eta \phi_\tau \rangle \quad (8)$$

$$= \langle \theta_\eta^2 \rangle + \alpha^2 \langle \phi_\tau^2 \rangle + \alpha^2 \frac{\sigma_n^2}{\tau} - 2\alpha \langle \theta_\eta \phi_\tau \rangle, \quad (9)$$

where we have assumed that the radiometer noise is uncorrelated with the phase signal, and that the radiometer noise decreases as the square root of the integration time. The w.v.r. phase is given by:

$$\phi_\tau = \frac{1}{\tau} \int_{-\tau/2}^{\tau/2} \theta(t') dt', \quad (10)$$

so we have terms such as:

$$\langle \phi_\tau \theta_\eta \rangle = \frac{1}{\tau\eta} \int_{-\eta/2}^{\eta/2} \int_{-\tau/2}^{\tau/2} \langle \theta(t_1) \theta(t_2) \rangle dt_1 dt_2. \quad (11)$$

Now, the autocorrelation function is assumed to be time independent, so that $\langle \theta(t_1) \theta(t_2) \rangle$ depends only on the time difference between t_1 and t_2 : *i.e.* $\langle \theta(t_1) \theta(t_2) \rangle = \xi(t_2 - t_1)$. We can therefore change variables, and by setting $x = t_2 - t_1$, $y = t_1 + t_2$, we get:

$$\langle \phi_\tau \theta_\eta \rangle = \frac{1}{2\tau\eta} \int \int \xi(x) dx dy, \quad (12)$$

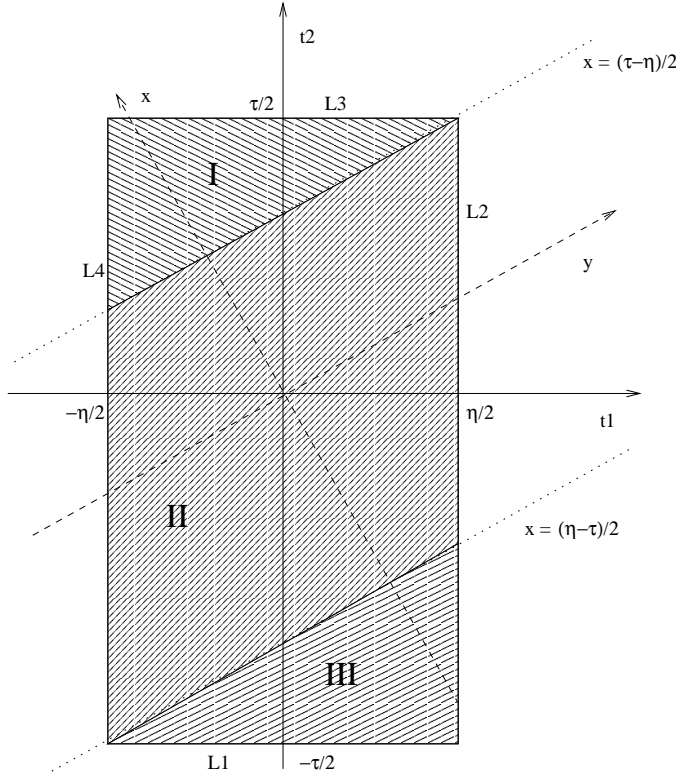


Figure 1: Changing coordinates of integration from t_1 and t_2 to $x = t_2 - t_1$, and $y = t_2 + t_1$.

where we have in effect rotated the axes of integration. The additional factor of two comes from the Jacobian of the transformation between (x, y) and (t_1, t_2) . Since this is a finite integration area, we need to consider the limits carefully. Figure 1 illustrates the change of coordinate system. While the limits are constant in the $t_1 - t_2$ coordinate space, these limits change along x and y . The limits can be found by breaking the area into three regions. In the first region (region I) the y limits lie between line L4 and L3. The second (region II) has y ranging between L4 and L2, and in the third region (region III) y lies between L1 and L2.

The equations of lines L1-4 are given by:

$$L1 : t_2 = -\tau/2; \quad L2 : t_1 = \eta/2; \quad L3 : t_2 = \tau/2; \quad L4 : t_1 = -\eta/2, \quad (13)$$

and using $x = t_2 - t_1$, and $y = t_1 + t_2$, we get:

$$L1 : y = -x - \tau; \quad L2 : y = \eta + x; \quad L3 : y = \tau - x; \quad L4 : y = x - \eta. \quad (14)$$

So the limits for y for regions I, II, and III are

$$I : x - \eta < y < \tau - x; \quad II : x - \eta < y < \eta + x; \quad III : -x - \tau < y < \eta + x, \quad (15)$$

and our corresponding limits for x are:

$$I : \frac{\tau - \eta}{2} < x < \frac{\tau + \eta}{2}; \quad II : -\frac{\tau - \eta}{2} < x < \frac{\tau - \eta}{2}; \quad III : -\frac{\tau + \eta}{2} < x < -\frac{\tau - \eta}{2}. \quad (16)$$

Integrating w.r.t. y , and using the limits defined in equations 15 and 16 we can rewrite equation 12 as:

$$\langle \phi_\tau \theta_\eta \rangle = \frac{1}{2\tau\eta} \int_{(\tau-\eta)/2}^{(\tau+\eta)/2} (\eta + \tau - 2x) \xi(x) dx + \frac{2\eta}{2\tau\eta} \int_{-(\tau-\eta)/2}^{(\tau-\eta)/2} \xi(x) dx + \frac{1}{2\tau\eta} \int_{-(\tau+\eta)/2}^{-(\tau-\eta)/2} (\eta + \tau + 2x) \xi(x) dx. \quad (17)$$

Making use of $\xi(-x) = \xi(x)$ to cast the third term's limits in the same form as the first term, this can be reduced to:

$$\langle \phi_\tau \theta_\eta \rangle = \frac{2}{2\tau\eta} \int_{(\tau-\eta)/2}^{(\tau+\eta)/2} (\eta + \tau - 2x) \xi(x) dx + \frac{4\eta}{2\tau\eta} \int_0^{(\tau-\eta)/2} \xi(x) dx. \quad (18)$$

So finally we are in a position to assemble an equation for the mean square error in phase correction using w.v.r. for a given correlation function. In order to make the final form (slightly) less messy, we can define two functions:

$$\mathcal{I}_1(a, b) = \int_0^{(a-b)/2} \xi(x) dx, \quad (19)$$

and

$$\mathcal{I}_2(a, b) = \int_{(a-b)/2}^{(a+b)/2} (a + b - 2x) \xi(x) dx, \quad (20)$$

then substituting for the terms in equation 7, the mean square error in the w.v.r. phase correction is given by:

$$\epsilon_\tau^2 = \frac{1}{\eta^2} \mathcal{I}_2(\eta, \eta) + \frac{\alpha^2}{\tau^2} \mathcal{I}_2(\tau, \tau) - 2\alpha \frac{1}{\tau\eta} \mathcal{I}_2(\tau, \eta) - 2\alpha \frac{2\eta}{\tau\eta} \mathcal{I}_1(\tau, \eta) + \alpha^2 \frac{\sigma_n^2}{\tau}. \quad (21)$$

To proceed from here, we need to choose an appropriate form for ξ , which we shall do in the next section.

5 Shape of structure function

The correlation function required for the calculations is for the phase variations as ‘seen’ by the antenna, and *once fast switching has been taken into account*. This differs from the ‘true’ correlation function both on small scales, where the antenna beam smooths out fluctuations on scales smaller than the size of the dish, and on large scales where the effect of fast switching is to remove phase variation on scales larger than the fast switching time interval. In this section we first consider the form of the atmospheric correlation function, and then describe how the antenna beam and fast-switching alter the correlation function.

5.1 Atmospheric fluctuations

In atmospheric flow that is fully turbulent, the structure function ($S(x)$, where $S(x) \equiv \langle [\phi(r) - \phi(r-x)]^2 \rangle$) can be described by a power law between scales ranging from a few cm up to a length scale set by the depth of the turbulent layer. On scales greater than the depth of the turbulent layer (l), the structure function turns over, and phases separated than more than l are expected to be uncorrelated. The depth of the turbulent layer is likely to depend on the time of day, being of order 100 m at night, and as high as 1 km during the daytime.

We assume here that we can model the shape of the structure function as a break between two power laws, giving a structure function that increases on small scales, and is constant above a certain length-scale, b , *i.e.* :

$$S(\Delta r) \equiv 2\sigma_\phi^2 - 2\langle \phi(r)\phi(r-\Delta r) \rangle = 2\sigma_\phi^2[1 - \xi(\Delta r)] \quad (22)$$

$$= 2\sigma_\phi^2 \frac{\Delta r^\gamma}{b^\gamma + \Delta r^\gamma}, \quad (23)$$

where b is the length-scale over which the fluctuations become decorrelated. The correlation function is then:

$$\begin{aligned} \xi(\Delta r) &= \sigma_\phi^2 - \frac{1}{2}S(\Delta r) \\ &= \sigma_\phi^2 \frac{b^\gamma}{b^\gamma + \Delta r^\gamma}. \end{aligned} \quad (24)$$

We can convert from spatial to temporal fluctuations by assuming that the fluctuations cross the antenna with constant velocity, V , and so $x = Vt$, *i.e.* :

$$\xi(\Delta t) = \sigma_\phi^2 \frac{(b/V)^\gamma}{(b/V)^\gamma + \Delta t^\gamma}. \quad (25)$$

While this correlation function gives the intrinsic atmospheric fluctuations, two modifications are required to take account of the antenna beam shape, and the use of fast-switching to a reference source.

5.2 Antenna beam shape

The antenna beam acts to smooth out small scale path length variations, on a scale of order the size of the antenna. We can treat this as a convolution of the original phases with a Gaussian of width corresponding to the time taken to cross half of the dish ($\sigma_d \sim 6\text{m}/V \text{ms}^{-1}$), *i.e.*

$$\phi' = \phi \star \exp[-t^2/2\sigma_d^2]. \quad (26)$$

In Fourier space this becomes:

$$\tilde{\phi}'_\omega = \sigma_d \tilde{\phi}_\omega \times \exp[-\omega^2 \sigma_d^2 / 2], \quad (27)$$

and so the power spectrum is given by:

$$P'(\omega) = \sigma_d^2 P(\omega) \exp[-\omega^2 \sigma_d^2]. \quad (28)$$

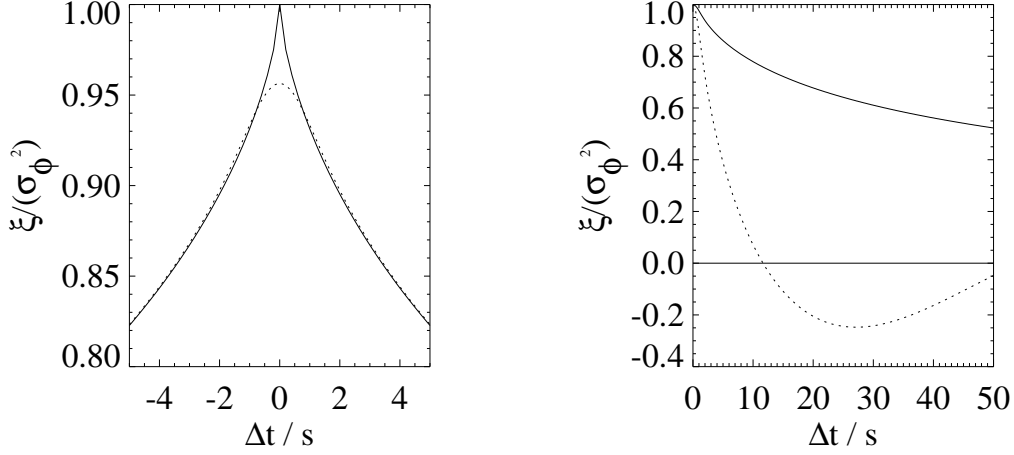


Figure 2: Left: The effect of antenna smoothing on the phase correlation function. Solid line shows the atmospheric correlation function before smoothing, and the dashed line shows the correlation function once it has been smoothed by the antenna beam. Right: The effect of fast-switching on the correlation function. Solid line shows the phase correlation function before fast-switching is applied, and the dashed line shows the correlation function after fast-switching has been applied, and after normalising to 1 at zero separation. In both cases, $\gamma = 2/3$ and $b/V = 50$ s were used to generate the initial correlation function from equation 25.

The corresponding correlation function is then

$$\begin{aligned}\xi'(t) &= \frac{1}{\sqrt{2\pi}} \int P'(\omega) \exp[i\omega t] d\omega \\ &\propto \xi(t) \star \exp[-t^2/4\sigma_d^2].\end{aligned}\quad (29)$$

The main effect of this smoothing is to flatten the correlation function close to $\Delta t = 0$, and this is shown in figure 2.

5.3 Fast switching

Fast switching provides an additional estimate for the atmospheric phase by pointing to a point source calibrator about once every 50 seconds. An estimate for the astronomical phase before fast switching is applied is given by:

$$\phi^{\text{source est}} = \phi^{\text{source}} + \phi^{\text{atmosphere}} - \phi^{\text{wvr}} - \phi^{\text{wvr noise}}, \quad (30)$$

and in Fourier space this is just:

$$\tilde{\phi}_\omega^{\text{source est}} = \tilde{\phi}_\omega^{\text{source}} + \tilde{\phi}_\omega^{\text{atmosphere}} - \tilde{\phi}_\omega^{\text{wvr}} - \tilde{\phi}_\omega^{\text{wvr noise}}. \quad (31)$$

The phase difference obtained when the antenna points at the calibrator is given by:

$$\phi^{\text{cal}} = \phi^{\text{atmosphere}} - \phi^{\text{wvr}} - \phi^{\text{wvr noise}}. \quad (32)$$

Now since this data is taken only every N seconds, only frequencies lower than π/N can be represented, and so in Fourier space, the calibration phase difference is given by:

$$\tilde{\phi}_\omega^{\text{cal}} = \left[\tilde{\phi}_\omega^{\text{atmosphere}} - \tilde{\phi}_\omega^{\text{wvr}} - \tilde{\phi}_\omega^{\text{wvr noise}} \right] \mathcal{H}_\omega(-\pi/N, \pi/N), \quad (33)$$

where \mathcal{H} is a top hat function:

$$\mathcal{H}_\omega(\pi/N, \pi/N) = \begin{cases} 0 & \text{for } \omega > \pi/N \text{ and } \omega < -\pi/N \\ 1 & \text{for } -\pi/N < \omega < \pi/N \end{cases}. \quad (34)$$

When the calibration phase is subtracted from the source estimate phase, in Fourier space we get:

$$\tilde{\phi}_\omega^{\text{source est}} - \tilde{\phi}_\omega^{\text{cal}} = \tilde{\phi}_\omega^{\text{source}} + \left[\tilde{\phi}_\omega^{\text{atmosphere}} - \tilde{\phi}_\omega^{\text{wvr}} - \tilde{\phi}_\omega^{\text{wvr noise}} \right] \left\{ 1 - \mathcal{H}_\omega(-\pi/N, \pi/N) \right\} \quad (35)$$

and so the effect of the fast switching (in the way it has been applied here) is to remove frequencies lower than $\omega = \pi/N$ from both the atmospheric phases and the w.v.r. data. This corresponds to a convolution of the atmospheric correlation function and radiometer output with the Fourier transform of $[1 - \mathcal{H}]^2 (= 1 - \mathcal{H})$. This acts to remove the largest-scale correlations, and effectively decreases the value of b in equation 23, so that the structure function rises more steeply, and turns over on a scale set by the fast switching time-scale, (if this is shorter than the coherence time-scale of the turbulent layer). This effect is shown in figure 2. The removal of large-scale power also acts to decrease the r.m.s. amplitude of the fluctuations and the amplitude of the radiometer noise, and so we take this into account in the analysis.

5.4 Typical phase statistics at Chajnantor

In this section we consider some realistic values for calculating the correlation function. Taking into account antenna beam smoothing and fast switching, the correlation function can be written as:

$$\xi(t) = \left[\sigma_\phi^2 \frac{(b/V)^\gamma}{(b/V)^\gamma + t^\gamma} \right] \star \left[\exp[-t^2 V^2 / 4\sigma_d^2] \right] \star \mathcal{FT} \left[1 - \mathcal{H}(-\pi/N, \pi/N) \right], \quad (36)$$

where \mathcal{FT} denotes the inverse Fourier transform, and \mathcal{H} is defined in equation 34.

Carilli, Lay & Sutton (1998; memo 210) suggested that typical exponents for the atmospheric structure function at Chajnantor were likely to be $\gamma = 5/3$ on baselines shorter than the thickness of the fluctuating layer, and $\gamma = 2/3$ for baselines greater than the thickness of the fluctuating layer. In addition, interferometric measurements of the r.m.s. phase fluctuations from Chajnantor (Butler *et al.*, 2001, memo 365; Evans *et al.*, 2003, memo 471) suggest that on 300 m baselines at 11.2 GHz the 10th percentile fluctuations are 1 degree at night, and 3 degrees during the day, while the 50th percentile fluctuations are 2 degrees at night, and 8 degrees during the day. These give r.m.s. path lengths of $\sigma_\phi = 75, 150, 220, 590 \mu\text{m}$ (for 1,2,3,8 degrees respectively).

The structure function turns over on scales of order the depth of the atmospheric boundary layer, and for these calculations we choose a value of $b = 500$ m. V is set to 10 m s^{-1} , and is chosen to be a characteristic wind speed at a height of 250 m.

The antenna beam size has a width of order half the size of the dish, and so we take $\sigma_d = 0.5$ s. Finally we assume that fast switching will take place every 50 s, so that $N = 50$. These values are summarised in table 1.

Once we have an estimate for the correlation function after beam smoothing and fast switching, we can use equation 21 to calculate how the error in w.v.r. phase correction depends on different smoothing times for the radiometer data (τ), and different weights for the radiometer data, α .

6 Results

Figure 3 shows how the r.m.s. residual path length, ϵ_τ , depends on τ and α for different values of γ and σ_ϕ . The dependence of τ and α on the r.m.s. path fluctuations, σ_ϕ , for different values of γ are shown in figure 4. For fluctuations of order 1 degree at 11.2 GHz ($75 \mu\text{m}$), an integration timescale of $\tau = 11$ s is preferred for three-dimensional Kolmogorov turbulence fluctuations ($\gamma = 5/3$), and $\tau = 3$ s for more two-dimensional turbulence ($\gamma = 2/3$). The optimum value of α is close to 1 for $\sigma_\phi > 100 \mu\text{m}$ for all values of γ , but for $\sigma_\phi < 100 \mu\text{m}$, the behaviour depends on γ , with the best fit value for α increasing for $\gamma = 5/3$, and decreasing for $\gamma = 0$. These dependences are discussed in greater detail below.

Dependence on σ_ϕ Figure 4 shows that the optimal smoothing time varies inversely with the r.m.s. phase, σ_ϕ , with the smoothing time required decreasing as σ_ϕ increases, and approaching a constant value for large σ_ϕ . This behaviour is set by the ratio of the radiometer noise to w.v.r. signal, since longer integration times reduce the noise, but increase the decorrelation between the atmospheric phases and the w.v.r. correction. As σ_ϕ decreases, the w.v.r. signal decreases relative to the noise, and a longer integration timescale is favoured to reduce the impact of the noise.

The variation of the best fit α with σ_ϕ is more complicated, and displays different behaviour for different values of γ . For $\sigma_\phi < 20 \mu\text{m}$ and $\gamma = \{2/3, 1, 5/3\}$, $\alpha > 1$ is favoured. In this regime the optimal integration time is very long, and this reduces the variance both of the noise term and of the w.v.r. signal relative to the measured atmospheric variance. An increased value of α therefore acts to compensate for the loss in variance of the w.v.r. signal.

For $\gamma = \{2/3, 1\}$, and in the range $20 < \sigma_\phi < 100 \mu\text{m}$, this behaviour switches quite steeply to a value of $\alpha < 1$. This is linked to the fall in integration time, which decreases the level of decorrelation between the w.v.r. time-averaged signal and the ‘true’ atmospheric phase, and increases the significance of the noise. The correction is therefore weighted down to reduce the impact of the noise from the radiometer.

For $\sigma_\phi > 100 \mu\text{m}$, the behaviour converges for all values of γ , and $\alpha \rightarrow 1$. In this regime, the w.v.r. signal dominates over the radiometer noise, and so using the actual w.v.r. measurement becomes favoured.

Dependence on γ Figure 4 also shows that the integration time is a strong function of the slope of the correlation function, γ . The difference in behaviour with γ is linked to the difference in the rate at which variance is lost when the fluctuations are smoothed over a given timescale. For low- γ distributions, the power is more evenly spread on different scales, whereas for high- γ distributions, the power tends to be concentrated in the larger-scale modes. Smoothing on a given timescale therefore tends to decrease the variance of the low- γ distributions more than for the high- γ distributions. While longer integration times bring the noise levels down, the longer the integration time, the larger the scales over which power is lost, and this has its biggest impact on the low- γ distributions. The tendency is therefore for low- γ distributions to favour smaller timescales of integration, and higher- γ distributions to favour longer timescales of integration.

σ_d / s	$\sigma_n / \mu\text{m}$	V / ms^{-1}	η / s	b / m
0.5	$10\sqrt{2}$	10	1	500

γ	$\sqrt{2}\sigma_\phi / \mu\text{m}$	$\tau \text{ best} / s$	$\alpha \text{ best}$	$\epsilon / \mu\text{m}$
1.67	25.	25.0	1.20	2.4
1.67	75.	10.6	1.03	4.3
1.67	150.	6.4	1.01	5.9
1.67	220.	5.1	1.01	6.7
1.67	590.	2.8	1.00	9.0
1.00	25.	10.8	0.97	4.6
1.00	75.	4.0	0.98	7.6
1.00	150.	2.7	1.00	9.3
1.00	220.	2.2	1.00	10.2
1.00	590.	1.5	1.00	12.1
0.67	25.	7.0	0.88	5.7
0.67	75.	2.8	0.97	9.0
0.67	150.	2.1	1.00	10.6
0.67	220.	1.8	1.00	11.4
0.67	590.	1.3	1.00	13.1

Table 1: Table showing the parameters used to generate the plots in figure 3. V is the horizontal velocity used to convert between spatial structure functions and a timeseries value, and is set to 10 ms^{-1} . $\sqrt{2}\sigma_\phi$ is the total r.m.s. path length fluctuation, and corresponds to the 10th and 50th percentile conditions during the day and during the night taken using an interferometer operating at 11.2 GHz on a 300 m baseline. For each value of γ and σ_ϕ , the best fit smoothing time, τ , and multiplicative factor, α , along with the expected minimum error in the correction, ϵ are shown.

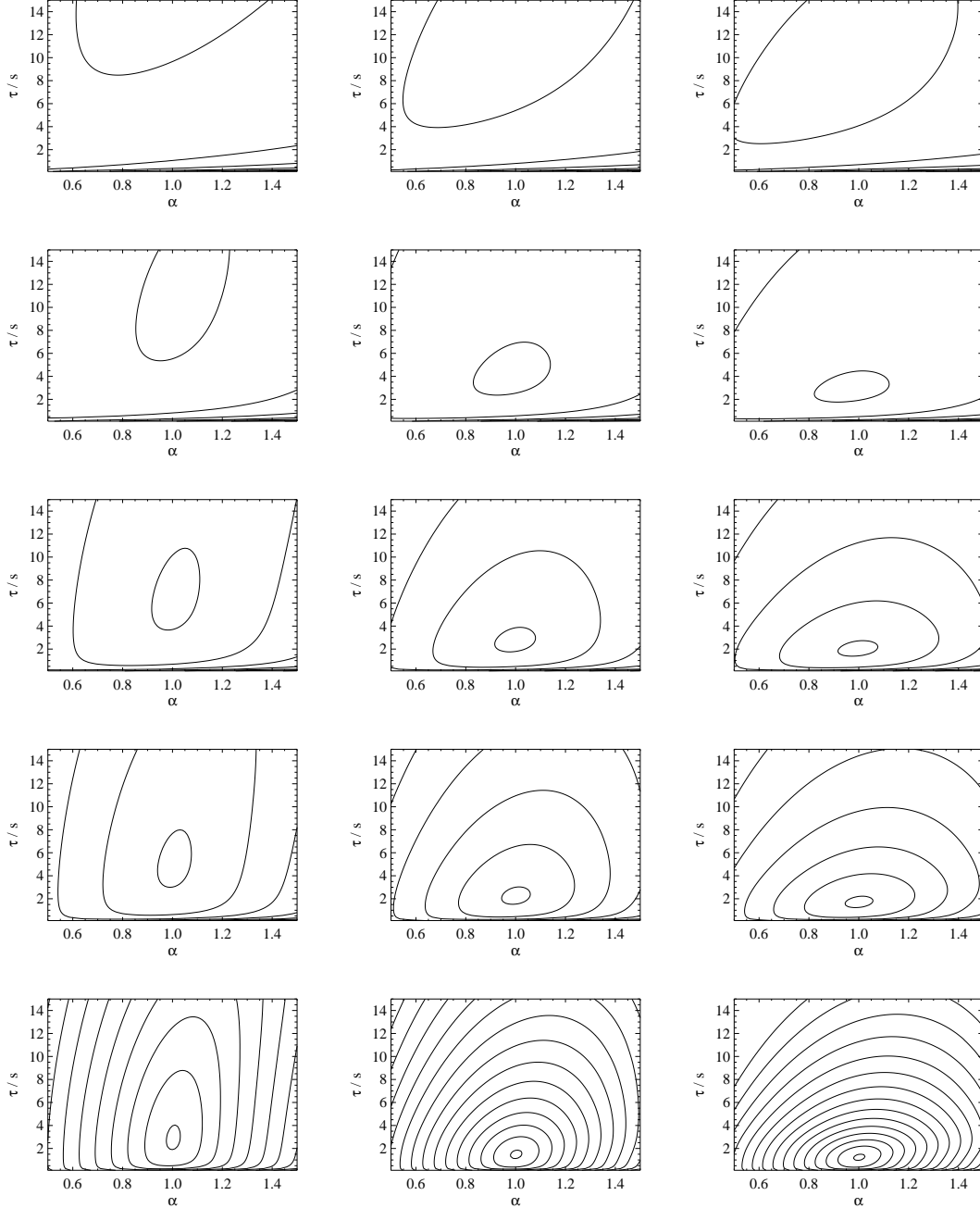


Figure 3: Contours of expected error in path once the w.v.r. correction has been taken into account, and as it varies with α and integration time, τ (see equations 7 and 10). Contours are at $10\mu\text{m}$ intervals, with the innermost contour at $1\mu\text{m}$ above the minimum point. (The minimum errors along with the best fit values for τ and α are recorded in table 1.) Each column has the same value of γ , and left to right, γ takes values $5/3$, 1 , and $2/3$. Each row has the same r.m.s. phase, σ_ϕ , measured in microns. Top row corresponds to an r.m.s. phase of $25\mu\text{m}$, and the second, third, fourth and fifth rows to 75 , 150 , 220 , and $590\mu\text{m}$ respectively. The other parameters are kept fixed and are listed in table 1.

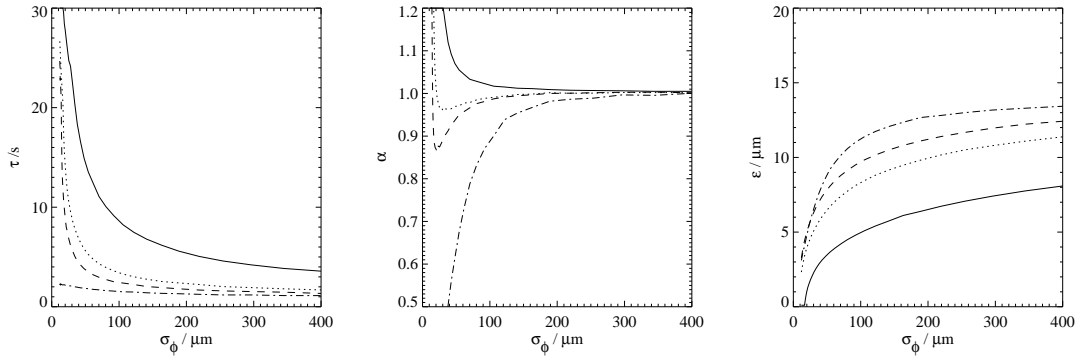


Figure 4: Left: The optimum integration time plotted against the r.m.s. phase fluctuations, σ_ϕ , for the best fit value of α , and different values of γ . Centre: the best fit value for α as it changes with σ_ϕ . For each value of σ_ϕ , the best fit τ is used. Right: the minimum error in correction, ϵ , as a function of σ_ϕ when the best fit values for τ and α are used. In each case, solid line is for $\gamma = 5/3$, dotted $\gamma = 1$, dashed $\gamma = 2/3$, and dot-dashed, $\gamma = 0$. Other parameters used are as listed in table 1.

7 Conclusions

In this memo we have looked at how w.v.r. measurements can be applied to correct for atmospheric phase fluctuations once fast switching has been applied. In particular we have calculated the optimum timescale over which the measurements should be averaged, and explored the possibility of allowing a multiplicative factor to reduce the impact of a noisy phase estimate on visibility data retrieved in good atmospheric conditions. Smoothing of the w.v.r. data causes a loss in resolution on smaller scales, but at the same time decreases the noise contribution.

We find that both the amplitude and slope of the spectrum of fluctuations influence the choice of timescale, and for typical fluctuations with r.m.s. $50 \mu\text{m}$ or more, and three-dimensional Kolmogorov turbulence, integration times of between 3 and 10 seconds are favoured. As the thickness of the turbulence layer becomes small compared with the size of the baseline, the turbulence becomes more two dimensional, and an integration time of between 1 and 3 seconds is preferred. The multiplicative factor in the conditions we have explored stays close to 1 until the atmospheric fluctuations drop below $\sim 100\mu\text{m}$, at which point a higher value is favoured for three-dimensional turbulence, and a lower value is preferred for two-dimensional turbulence.

While we have not directly addressed the impact of dry fluctuations in this memo, in circumstances where these are uncorrelated with the wet fluctuations, the above analysis would be expected to hold. When there is a certain amount of correlation between the dry and wet fluctuations, the factor α could be used to increase or decrease the w.v.r. estimate accordingly.

Finally, an issue raised by this report is how this approach may be applied in practice. For instance, should we decide what the w.v.r. averaging time should be as the data is collected? One possible approach would be to collect both the w.v.r. and interferometer data in a buffer of similar size to the final averaging time (30-60 s). The data in this buffer could be used to measure the w.v.r. fluctuations, and infer the phase fluctuations above

each antenna. In cases where one might use the same averaging time for each antenna (for example in compact configurations, or when the atmosphere is very stable), the averaging time could be calculated from the r.m.s. w.v.r. fluctuation level, or from the average temporal structure function of each w.v.r.. This would allow the averaging times to change every 30-60 seconds. Clearly, it would be important to store the averaging time alongside the data to facilitate any additional corrections that might need to be made. While there may sometimes be a case for applying different w.v.r. averaging times at each antenna, for instance when ALMA is in a large configuration, application in real time would be complicated, and should perhaps be avoided unless it can give a large improvement to the phase correction.

8 References

- Butler, B.J., Radford, S.J.E., Sakamoto, S., Kohno, K., 2001, ALMA Memo 365, 'Atmospheric phase stability at Chajnantor and Pampa la Bola'
- Hills, R.E., 2004, 'Estimated performance of the water vapour radiometers, ALMA Memo 495'
- Carilli, C.L., Lay, O., Sutton, E.C., 1998, MMA Memo 210, 'Radiometric phase correction'
- Evans, N., Richer, J.S., Sakamoto, S., Wilson, C., Mardones, D., Radford, S., Cull, S., Lucas, R., 2003, ALMA memo 471, 'Site properties and stringency'
- Stirling, A.J., Hills, R.E., Richer, J.S., Pardo, J.R., 2004, ALMA Memo 496, '183 GHz water vapour radiometers for ALMA: Estimation of phase errors under varying atmospheric conditions'
- Thompson, A.R., Moran, J.M., Swenson, G.W., 2001, *Interferometry and Synthesis in Radio Astronomy*, 2nd ed, Wiley Interscience. Williamson R., Hills, R.E., 2004, DRD04 – Design report, WVR PDR documentation package